DOI 10.5162/Ultrasonic2025/E5-a2

Elliptical polarization and irrotational characteristics of inhomogeneous plane elastic longitudinal waves

Hengshan Hu[1], *Tian Lin*[1], *and Wei Guan*[1]
[1]*Harbin Institute of Technology, Harbin, Heilongjiang, China*
hhs@hit.edu.cn

Abstract: When a homogeneous plane longitudinal or P-wave in a fluid is incident on a fluid-solid interface at a supercritical angle, it generates an inhomogeneous refracted P-wave in the elastic solid. In this study an inhomogeneous elastic P-wave is demonstrated to have components parallel to and perpendicular to the direction of propagation, exhibiting elliptical polarization characteristics. While the wavefield remains irrotational, the traveling velocity along the propagation direction is slightly less than that of a homogeneous P-wave.

Keywords: longitudinal wave, inhomogeneous wave, polarization, elastic medium, borehole.

Introduction

When discussing P-waves, the common perception is that particle displacement aligns with the propagation direction—a characteristic indeed true for homogeneous plane P-waves. However, inhomogeneous P-waves propagating along elastic medium interfaces (or surfaces) exhibit nonuniform amplitude distribution across wavefronts, with amplitudes decaying as distance from the interface/surface increases [1]. This raises the question: Does particle displacement in inhomogeneous elastic P-waves remain parallel to the propagation direction?

In elastic media, inhomogeneous waves are often termed evanescent, decaying, or vanishing waves. Inhomogeneous plane P-waves commonly occur near interfaces or surfaces, such as "glide" P-waves in acoustic logging [2] and P-head waves at the seafloor in marine exploration [3]. The P- and S-waves measured in acoustic logging propagate axially along the borehole wall before returning to the wellbore, traveling at speeds close to those of body waves in homogeneous media. Some scholars refer to them as "glide P-wave" and "glide S-wave" [4]. The glide P-wave is also known as primary head wave, while the glide S-wave is known as secondary head wave. Chen et al. [5] observed that glide P-waves possess both axial and radial displacement components.

These studies indicate that the borehole P-wave differs significantly from the homogeneous P-wave in a unbounded medium. Here we focus our attention on the properties of the refracted inhomogeneous P-wave generated at fluid-solid interface.

Inhomogeneous Refracted P-Waves at a Fluid-Solid Interface

Consider a homogeneous plane P-wave obliquely incident from a fluid half-space to a solid half-space

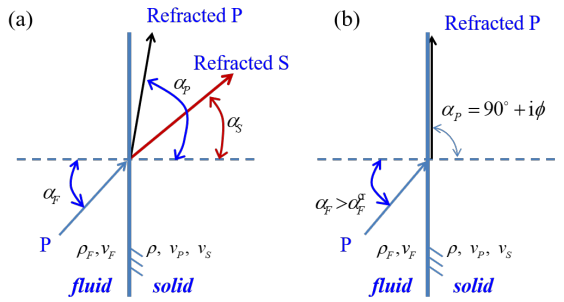

Fig. 1: Schematic of refraction on a fluid-solid boundary. (a) at small incident angle, (b) at supercritical incident angle.

(Fig. 1a). Here both the fluid and the solid are assumed to be perfectly elastic.

Wave conversions on the boundary obey Snell's law

$$\frac{\sin\alpha_P}{v_P} = \frac{\sin\alpha_F}{v_F}, \tag{1}$$

where v_F is P wave velocity in the fluid, v_P and v_S are P and S wave velocities in the solid. α_F is the incident angle in the fluid side. α_P and α_S are respectively the angles of refraction P and S waves. It is assumed that $v_P > v_F$, so that $\alpha_P > \alpha_F$. When $\alpha_P = 90°$, the P wave in the solid is critically refracted and travels along the boundary. In that case, the incident angle is

$$\alpha_F^{\rm cr} = \sin^{-1}\frac{v_F}{v_P}. \tag{2}$$

When the incidence angle becomes larger than the critically incidence angle, as in Fig. 1b, Eq. (1) remains valid and

$$\sin\alpha_P = \frac{v_P}{v_F}\sin\alpha_F > \frac{v_P}{v_F}\sin\alpha_F^{\rm cr} = 1. \tag{3}$$

DOI 10.5162/Ultrasonic2025/E5-a2

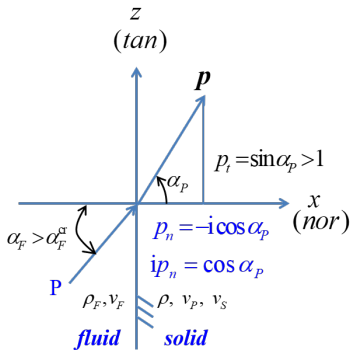

Fig. 2: The complex refraction angle and the complex propagation vector

The angle of the refracted P wave, α_P, must be a complex number, with the real part being $\pi/2$, i.e.,

$$\alpha_P = 90^\circ + \mathrm{i}\phi. \tag{4}$$

Now $\cos\alpha_P$ is a pure imaginary number because

$$\cos\alpha_P = \sqrt{1-\sin^2\alpha_F} = \mathrm{i}\sqrt{\sin^2\alpha_F - 1}. \tag{5}$$

The sign of square root is so chosen that the wave amplitude decreases with the depth into the solid, as will be seen in the next section. As depicted in Fig. 2, the propagation vector $\boldsymbol{p}$ has a tangential component p_t of real value and a normal component $\mathrm{i}p_\mathrm{n} = \mathrm{i}\sqrt{\sin^2\alpha_F - 1}$, with

$$p_\mathrm{t} = \sin\alpha_P > 1, \tag{6}$$

$$p_\mathrm{n} = -\mathrm{i}\cos\alpha_P = \sqrt{\sin^2\alpha_P - 1} > 0, \tag{7}$$

so that

$$\boldsymbol{p} = \boldsymbol{e}_t \sin\alpha_p + \boldsymbol{e}_n \cos\alpha_p = p_t\boldsymbol{e}_t + \mathrm{i}p_n\boldsymbol{e}_n. \tag{8}$$

Expressing in the form of plane harmonic wave, the displacement is

$$\begin{aligned}\boldsymbol{u} &= A\boldsymbol{d}\exp\left[\mathrm{i}k(\boldsymbol{p}\cdot\boldsymbol{x} - v_p t)\right] \\ &= A\boldsymbol{d}\exp\left[\mathrm{i}k(p_t z + \mathrm{i}p_n x - v_p t)\right] \\ &= A\boldsymbol{d}\exp\left(-kp_n x\right)\cdot\exp\left[\mathrm{i}k(p_t z - v_p t)\right],\end{aligned} \tag{9}$$

where A is the amplitude factor, k is the wavenumber. From Eq. (9) it is clear that the displacement decays exponentially with the depth x normal to the interface, the refracted P-wave is thus called inhomogeneous. It propagates with a tangential velocity

$$v_\mathrm{t} = \frac{dz}{dt} = \frac{v_P}{p_\mathrm{t}} = \frac{v_P}{\sin\alpha_P} < v_P, \tag{10}$$

in which Eq. (6) is used. Eq. (10) tells us that the tangential phase velocity v_t is less than the homogeneous P-wave velocity.

When a homogeneous P-wave in a fluid is obliquely incident on the fluid-solid interface with the incidence angle larger than critical incidence angle, the angle of refraction will be a complex value, and the refracted wave in the elastic sold half-space travels with a tangential velocity less than the P-wave velocity in the medium, and with an amplitude decreasing with the depth normal to the interface.

Polarization feature of the refracted inhomogeneous P-waves

In this section, we discuss particle displacement pattern in the refracted inhomogeneous P-wave field. Achenbach [1] proved that a plane wave in the time domain expressed by Eq. (11)

$$\boldsymbol{u} = \boldsymbol{d}f(\boldsymbol{p}\cdot\boldsymbol{x} - ct) \tag{11}$$

is irrotational as long as

$$\boldsymbol{d} = \boldsymbol{p} \tag{12}$$

and

$$\boldsymbol{p}\cdot\boldsymbol{p} = 1 \tag{13}$$

Here, we point out that Eq. (13) does not require the a complex propagation vector $\boldsymbol{p}$ is of unit length. In fact, when $\boldsymbol{p} = \boldsymbol{p}_R + \mathrm{i}\boldsymbol{p}_I$, Eq. (13) leads to

$$\boldsymbol{p}_R\cdot\boldsymbol{p}_I = 0, \tag{14}$$

$$\boldsymbol{p}_R\cdot\boldsymbol{p}_R - \boldsymbol{p}_I\cdot\boldsymbol{p}_I = 1, \tag{15}$$

in which $\boldsymbol{p}_R$ and $\boldsymbol{p}_I$ are respectively real and imaginary parts of the propagation vector. In our expression for super-refracted P wave, the propagation vector described by Eq. (8) satisfies Eq. (13), with $\boldsymbol{p}_R = \boldsymbol{e}_t p_t = \boldsymbol{e}_t\sin\alpha_p$, $\boldsymbol{p}_I = \boldsymbol{e}_n p_n = \boldsymbol{e}_n\sqrt{\sin^2\alpha_p - 1}$, and $p_t^2 - p_n^2 = 1$. The super-refracted P wave is irrotational as long as $\boldsymbol{d} = \boldsymbol{p}$.

Rewriting Eq. (9) as

$$\begin{aligned}\boldsymbol{u} &= A(\boldsymbol{p}_R + \mathrm{i}\boldsymbol{p}_I)\exp(-kp_n x)\cdot\exp\left[\mathrm{i}k(p_t z - v_p t)\right] \\ &= A(\boldsymbol{e}_t p_t + \mathrm{i}\boldsymbol{e}_n p_n)\exp(-kp_n x)\cdot\exp\left[\mathrm{i}k(p_t z - v_p t)\right].\end{aligned} \tag{16}$$

The tangential and normal components are respectively

$$u_t = Ap_t\exp(-kp_n x)\cdot\exp\left[\mathrm{i}k(p_t z - v_p t)\right], \tag{17}$$

$$u_n = \mathrm{i}Ap_n\exp(-kp_n x)\cdot\exp\left[\mathrm{i}k(p_t z - v_p t)\right]. \tag{18}$$

Their real parts are

$$\mathrm{Re}(u_t) = Ap_t\exp(-kp_n x)\cdot\cos\left[k(p_t z - v_p t)\right], \tag{19}$$

$$\mathrm{Re}(u_n) = -Ap_n\exp(-kp_n x)\cdot\sin\left[k(p_t z - v_p t)\right]. \tag{20}$$

DOI 10.5162/Ultrasonic2025/E5-a2

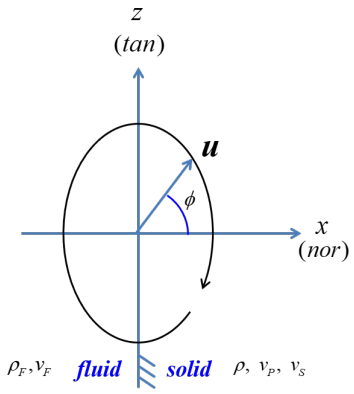

Fig. 3: The trajectory of refracted P-wave displacement at $z = 0$ on the boundary.

It is obvious that

$$\frac{[\mathrm{Re}(u_t)]^2}{[Ap_t \exp(-kp_n x)]^2} + \frac{[\mathrm{Re}(u_n)]^2}{[Ap_n \exp(-kp_n x)]^2} = 1. \tag{21}$$

Because $p_t > 1$ and $p_n = \sqrt{\sin^2 \alpha_p - 1} < p_t$, the trajectory of the displacement of a particle on the boundary is elliptic, with the long axis being in the tangential direction. Specifically, the trajectory shape changes with the incidence angle α_F, so that

$$\frac{[\mathrm{Re}(u_t)]^2}{A^2 \left(\frac{v_p}{v_F}\right)^2 \sin^2 \alpha_F \mathrm{e}^{-2kp_n x}} + \frac{[\mathrm{Re}(u_n)]^2}{A^2 \left(\left(\frac{v_p}{v_F}\right)^2 \sin^2 \alpha_F - 1\right) \mathrm{e}^{-2kp_n x}} = 1, \tag{22}$$

in which p_n also depends on α_F because $p_n = \sqrt{\left(\frac{v_P}{v_F}\right)^2 \sin^2 \alpha_F - 1}$. The displacement vector of a particle on the boundary goes clockwise as shown in Fig. 3.

The trajectory is similar to the Rayleigh wave on the surface of an elastic half-space. The Rayleigh wave is well known as a combination of an inhomogeneous P wave and an inhomogenous S wave. It travels with a velocity less than that of the shear wave in the medium. Now we see that the displacement of a homogenous P-wave itself goes with an elliptic trajectory, with the long axis in the tangential direction, and the short axis normal to the interface.

Discussions

The super-refracted P-wave has a tangential velocity smaller than the P-wave velocity of the formation. The recorded P-wave in acoustic logging is composed of inhomogeneous P-wave generated when the incident angle exceeds the critical incidence angle. Although critical refraction does occur at exact critical incidence angle, the acoustic energy associated with a cone of the zero thickness might be negligible. It is reasonable to conclude that the observable P-wave is inherently associated with inhomogeneous P-wave, so that the picked up velocity by commonly used slowness-time coherence method [6] will inevitably be slower than the real P-wave velocity of the formation. We suggest a correction scheme be provided after careful investigation.

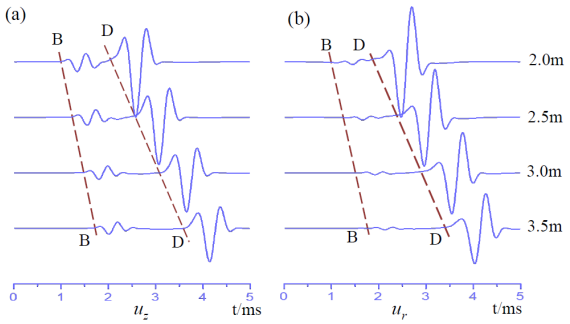

Fig. 4: Waveforms of displacement components at the borehole wall in a slow formation

We would like to point out that the Snell's law is in fact a part of the conclusions drawn from boundary conditions. It is the incident wave and all outgoing waves combining together that satisfies the boundary conditions. The refracted S-wave is among the outgoing waves as long as the incidence angle is nonzero.

When investigating waves excited by an acoustic monopole source in a borehole, Hu [7] calculated the z-axial and radial components of the displacement on the borehole wall in a slow formation with $v_P = 2331\,\mathrm{m/s}$, $v_S = 1083\,\mathrm{m/s}$, $\rho = 2259\,\mathrm{kg/m^3}$. The density and acoustic velocity in the fluid are respectively $\rho_F = 1000\,\mathrm{kg/m^3}$ and $v_F = 1500\,\mathrm{m/s}$. In his result, both the radial displacement and the axial displacement exhibit a disturbance with the P-wave velocity, as in Fig. 4.

Two facts can be used to explain the waveform of u_r in Fig. 4b. The normal displacement waveform exhibits a disturbance with an approximate P-wave velocity because the glide P-wave is actually elliptically polarized, with a normal displacement component as well as a tangential one. Besides, refracted S-wave is generated whenever the incidence angle is nonzero.

Similarly, refraction S-wave will have a complex angle when the incidence angle in the fluid is greater than the second critical incidence angle. The super-refracted S-wave is also inhomogeneous and has a tangential velocity smaller that the S-wave velocity of the formation. It causes tangential displacement as

well as normal displacement. The displacement trajectory can be similarly analyzed. The displacement of a inhomogeneous S-wave goes along an elliptic trajectory, with the short axis in the tangential direction, and the long axis normal to the interface.

Conclusion

Inhomogeneous refracted P-wave is generated in the formation when the incidence angle in the fluid is larger than critical incidence angle. While it remains an irrotational wave, it travels along the interface with a velocity slower than that of P-wave in a unbounded medium. Its displacement has a normal component as well as a tangential displacement. For a particle on the interface, the displacement vector of the inhomogeneous refracted P wave goes clockwise along an elliptic trajectory, with the long axis being in the tangential direction. Different than the Rayleigh wave, the inhomogeneous P wave has a traveling velocity slightly lower than that in a unbounded medium.

Discussed here is about waves in perfect elastic medium. The conclusions here can be drawn from the more general theory on inhomogeneous waves in viscoelastic media as expounded by Borcherdt [8] in 2009. In spite of being so, our presentation on inhomogeneous waves in perfect elastic medium is easier to understand. We expect it to be beneficial to borehole geophysicists for understanding the wave mechanism of the glide P and S waves on a borehole wall.

Acknowledgments

We acknowledge the financial support by the National Science Foundation of China (NSFC-12472087 and NSFC-12272107).

References

[1] J. D. Achenbach. *Wave Propagation in Elastic Solids*. Amsterdam/New York: North - Holland Publishing Company/American Elsevier, 1973.

[2] Q. Dong, K. Wang, C. Luo, et al. "Resonance and attenuation of the head wave in a fluid - filled borehole". In: *Chinese Journal of Geophysics* 34.02 (1991), pp. 228–239.

[3] J. M. Carcione. *Wave fields in real media: wave propagation in anisotropic, anelastic, porous and electromagnetic media*. 3nd. Amsterdam/New York: Elsevier Science, 2011.

[4] J. Zhang. "Detection depth of acoustic velocity logging". In: *Well Logging Technology* 5.06 (1981), pp. 64–67.

[5] W. Chen, Z. Chu, S. Wang, et al. "Theoretical and Experimental Study on Acoustic Frequency Spectrum Log in a Well Model". In: *Well Logging Technology* 22.06 (1998), pp. 3–11.

[6] C. Kimball and T. Marzetta. "Semblance processing of borehole acoustic array data". In: *Geophysics* 49.3 (1986), pp. 274–281.

[7] H. Hu. "Acoustic head wave on the borehole wall in a porous formation and the causes for its accompanying electromagnetic field". In: *Acta Physica Sinica* 52.8 (2003), pp. 1954–1959.

[8] R. Borcherdt. *Viscoelastic Waves in Layered Media*. New York: Cambridge University Press, 2009.